Mitigation of indoor low-frequency noise using single channel active noise control system

Ken KANEUCHI[1]; Koichi NISHIMURA[2]; Toshihito MATSUI[3]

[1, 2] OSAKA GAS CO., LTD, Japan

[3] Hokkaido University, Japan

ABSTRACT

In an enclosed space such as a residential space, noise transmitted from outside is amplified at the resonant frequency of the indoor space. The resonant frequency of a residential space is generally close to the low frequency sound of 200 Hz or less. In this study, a single channel active noise control system that has only one secondary source was evaluated experimentally for mitigating low frequency resonance. A standing wave that causes resonance was canceled out by the one secondary source. The similar results were also obtained by numerical simulation utilizing the boundary element method. The simulation is used for arranging an optimal position of active noise control system. From this study, it was confirmed that the single channel active noise control system can mitigate indoor low frequency noise on loops of standing wave efficiently.

Keywords: Active noise control, Standing wave, Low frequency noise I-INCE Classification of Subjects Number(s): 02.1

1. INTRODUCTION

Rotary machines such as fans and pumps emit noise with a peak at a specific frequency depending on the rotating speed of the machine. In an enclosed space such as a residential space, noise transmitted from outside is amplified at the resonance frequency of the indoor space. If the frequency of the noise and the resonant frequency of the space are close in value, the noise may increase excessively and cause discomfort to occupants. The resonant frequency of a residential space is generally close to the low-frequency sound of 200 Hz or less. However conventional methods of suppressing noise using passive sound absorption materials and barriers are not effective against low-frequency noise. Therefore, Active Noise Control (ANC) which is an effective method for reducing low-frequency noise (1) is the focus of this study.

The ANC is practically used for ear phones, ducts and automobiles (2), but not used in wide space such as residential rooms. There has been a study for reducing low-frequency noise in enclosed sound field. For example, methods to minimize averaged acoustic energy by multiple secondary sources are researched(3). In residential rooms, Hiruma and Enamito studied about sound field control technology which is confined to the sound field around the listener(4). ANC is installed at openings, such as window, for canceling out noise through openings(5). However, it is confined to narrow openings. If the opening is wide, multiple secondary sources are needed. For controlling sound field, multi-channel control is often needed. For application to residential rooms, a simple system is practical. If targets are limited to low-frequency noise, which is enhanced by standing wave, a single channel ANC system can decrease the noise in the room efficiently(6).

In this study, a single channel ANC system with one secondary source was evaluated experimentally for mitigating low-frequency noise, which is enhanced by a standing wave.

[1] k-kaneuchi@osakagas.co.jp
[2] nishimur@osakagas.co.jp
[3] t.matsui@eng.hokudai.ac.jp

2. EIGENMODES OF SOUND FIELD

This study aimed at reducing low-frequency noise , which is enhanced by resonance in the residential room. At first, eigenmodes of target sound field were checked experimentally.

A primary source was installed at out of the room, because target of this study is noise transmitted from outside. Sound pressure was measured in a rectangular-shaped room whose dimension is 5.43m in width, 7.18m in length, and 2.65m in height as shown in Fig.1. The walls of the room are composed by mainly concrete. An average absorption rate measured by the reverberation room method is 0.015 at 50Hz. It is confirmed that the sound easily reverberates in the room. Room temperature was adjusted to 25 degrees Celsius by air conditioning during the experiment. In the room, sound pressure was measured at 9 points toward x-axis, 11 points toward y-axis as shown in Fig.1, and 5 points toward z-axis for a total of 495 points. Sound pressure near the primary source in outdoor and vibration acceleration on the windows was measured for comparing to sound pressure in the room. Vibration acceleration was measured at 52 points as shown in Fig.2. For checking the sound field in the room, white noise was generated from the primary source.

Spector level of the sound pressure near the primary source in outdoor, mean-square vibration acceleration on the windows, and mean-square sound pressure in the room are shown in Fig.3. In the room, there were peaks that did not exist at outside sound pressure and windows vibration, indicating that sound pressure was enhanced at modal frequencies in the room. If the direction of x, y, and z are defined in the room space as shown in Fig.1, the resonant frequencies of the room f are calculated by eqn. (1). The terms l_x, l_y, and l_z specifies the length of each axis of the room, n_x, n_y, and n_z specifies the eigenmodes of each axis, and c specifies sound velocity.

$$f = \frac{c}{2}\sqrt{\left(\frac{n_x}{l_x}\right)^2 + \left(\frac{n_y}{l_y}\right)^2 + \left(\frac{n_z}{l_z}\right)^2} \tag{1}$$

Table 1 shows the resonant frequencies calculated by eqn.(1) and the peak frequencies of sound pressure as confirmed in Fig. 3. As shown in Table 1, the peak frequency of indoor sound pressure is largely similar to the theoretical value calculated using eqn. (1). Distribution of sound pressure levels at 50Hz, 69Hz, 74Hz, and 82Hz on the floor of the room are shown in Fig.4. Experimental eigenmodes which were confirmed from Fig.4 closely coincide with theoretical eigenmodes.

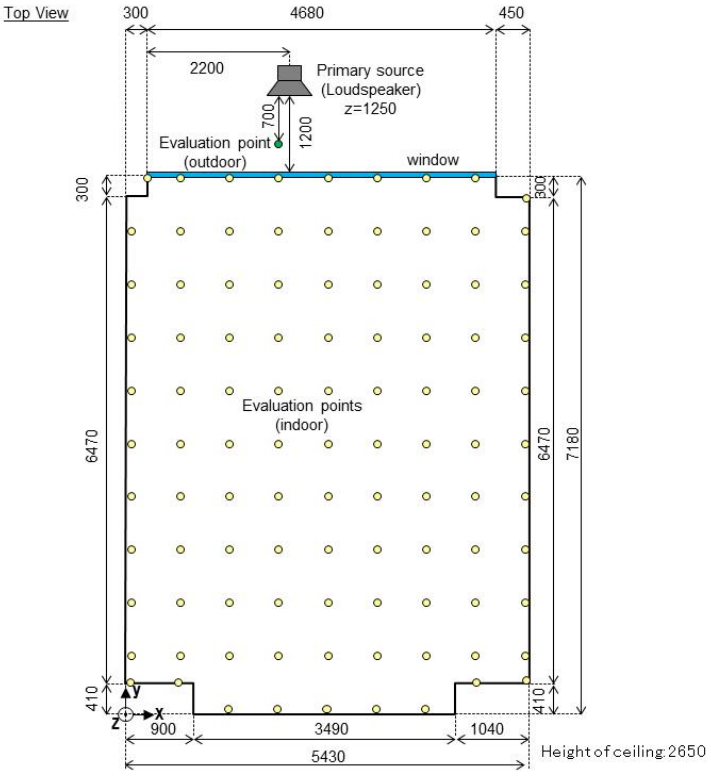

Figure 1 –Geometry of the room used for experimentation and layout of the primary source and evaluation points.

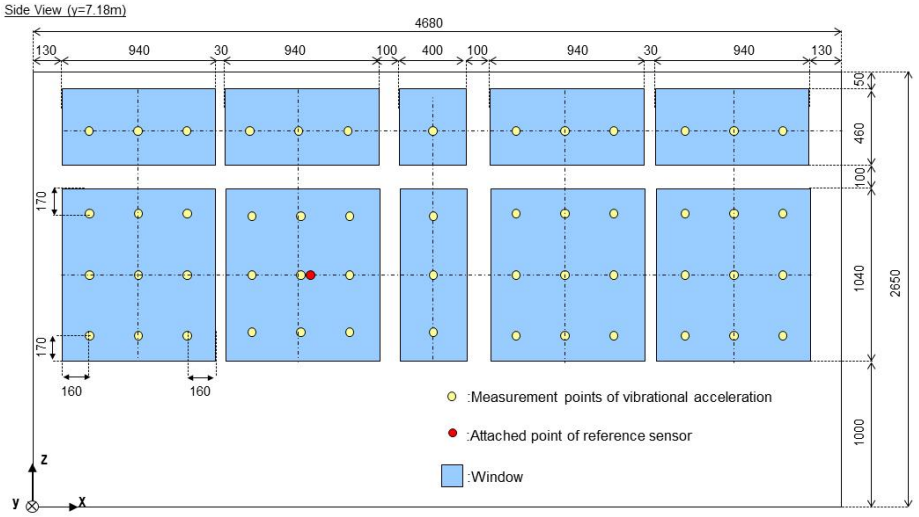

Figure 2 –Geometry of window and position of measurement points of vibration acceleration.

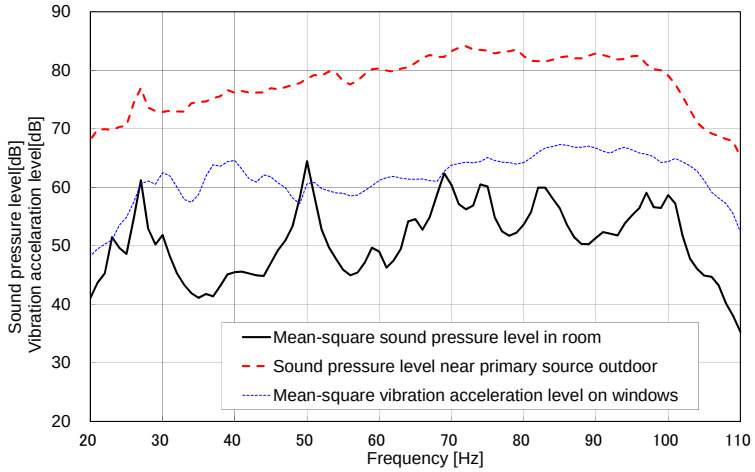

Figure 3 –Spector level of sound pressure and vibration acceleration.

Table 1 – Eigenmodes of each axis and resonant frequency in the room

Eigenmodes of each axis			Resonant frequency	
n_x	n_y	n_z	Theoretical value	Experimental value
0	1	0	24.1	27
1	1	0	40.0	-
0	2	0	48.3	50
1	2	0	57.9	59
2	0	0	63.9	65
2	1	0	68.3	69
0	3	0	72.4	74
2	2	0	80.1	82
2	3	0	96.6	97

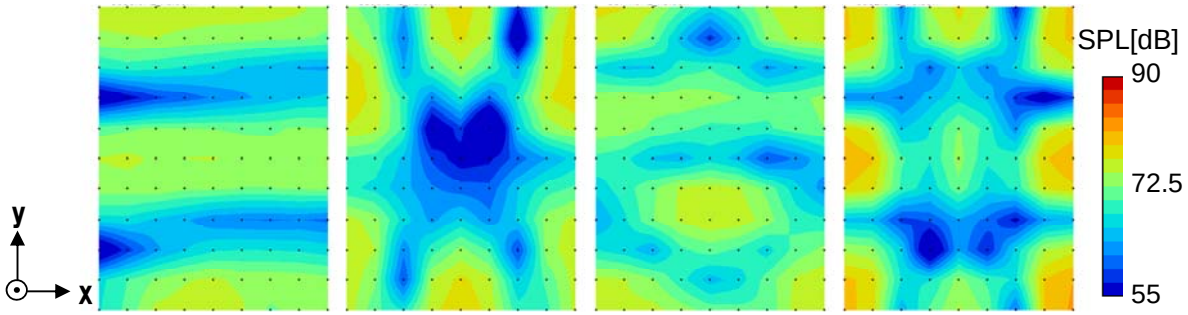

Figure 4 –Distribution of sound pressure level on floor (50Hz, 69Hz, 74Hz, and 82Hz)

3. NUMERICAL SIMULATION

3.1 Calculation Method

The performance of the ANC system is dependent on the position of the secondary source and the error sensor. In this study, numerical simulation utilizing Boundary Element Method (BEM) was used for arranging a position of the ANC system. At first, the sound field of the room was calculated using the same experimental conditions to validate calculation accuracy. Boundary conditions for vibrating boundary and absorbing boundary were set as follows. The boundary integral equation for calculating pressure at point *i* is shown as eqn. (2). If the boundary was divided into *N* elements as shown in Fig.5, discretized equation is shown as eqn. (3)

$$Cp_i = \int_s G \frac{\partial p}{\partial n} ds + \int_s \frac{\partial G}{\partial n} p ds \tag{2}$$

$$Cp_i = \sum_{m=1}^{N} \int_{s_m} G \frac{\partial p_m}{\partial n} ds + \sum_{m=1}^{N} \int_{s_m} \frac{\partial G}{\partial n} p_m ds \tag{3}$$

N specifies total number of elements, *s* specifies area, *p* specifies pressure, and *G* specifies green's function. *C* is the value obtained when the internal solid angle is divided by 4π. Green's function of 3-dimentional Helmholtz equation *G* and the normal derivative equation of *G* are shown in eqn. (4) and eqn. (5), respectively.

$$G = -\frac{1}{4\pi r} e^{-ikr} \tag{4}$$

$$\frac{\partial G}{\partial n} = -\frac{1 + jkr}{4\pi r^2} e^{-ikr} \frac{\partial r}{\partial n} \tag{5}$$

The term *r* specifies the distance between point *i* and element *m*, *k* specifies wave number, and *n* specifies normal vector. If the vibration acceleration on the boundary element was known, the boundary element was treated as a Neumann boundary condition as shown in eqn. (6)

$$\frac{\partial p_m}{\partial n} = -j\omega\rho u_m = -j\rho a_m \tag{6}$$

The term u_m specifies the particle velocity at element *m*, and a_m specifies vibration acceleration at element *m*. The measured values on windows were used for a_m. The term ω specifies angular frequency and ρ specifies air density. The boundary condition of the windows was treated as a Neumann problem. Figure 6 shows distribution of measured vibration acceleration level on windows.

Boundaries whose absorption rate are known were treated as a Robin boundary condition, which was stipulated by relation of p_m and the normal derivative p_m as shown in eqn. (7)

$$\frac{\partial p_m}{\partial n} = -jkAp_m \tag{7}$$

The term *A* specifies the acoustic admittance ratio. *A* was derived from the absorption ratio α as shown in eqn. (8).

$$A = \frac{1 - \sqrt{1-\alpha}}{1 + \sqrt{1-\alpha}} \tag{8}$$

It was assumed that all boundaries except windows were treated as Robin boundary conditions. Absorption rates measured by the reverberation room method were used. Absorption rates at resonant frequencies in the room are shown Table 2. For confirming sound field of the room, pressure was calculated at 25cm intervals in a total number of 6,809 points in the room. Figure 7 shows the distribution of calculated sound pressure level on the floor. As shown in Fig.4 and Fig.7, the calculated distribution of the sound pressure level was coincident with experimental distribution. It was confirmed that BEM simulation can be used for predicting sound fields.

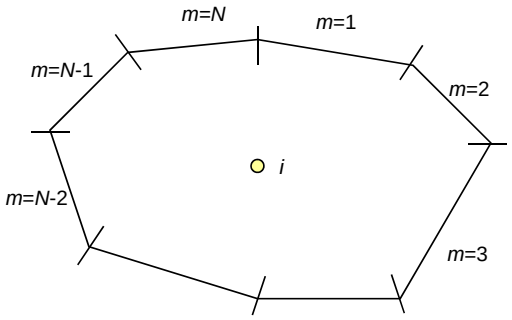

Figure 5 –Divided boundaries

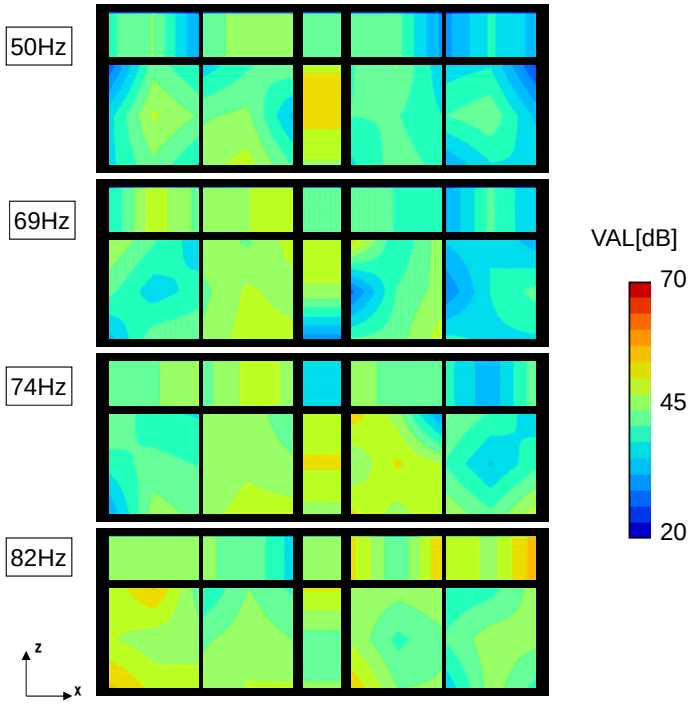

Figure 6 –Distribution of vibration acceleration level on windows (50Hz, 69Hz, 74Hz, and 82Hz)

Table 2 – Absorption rates at resonant frequencies in the room.

Frequency	Absorption rate
50	0.015
69	0.03
74	0.03
82	0.04

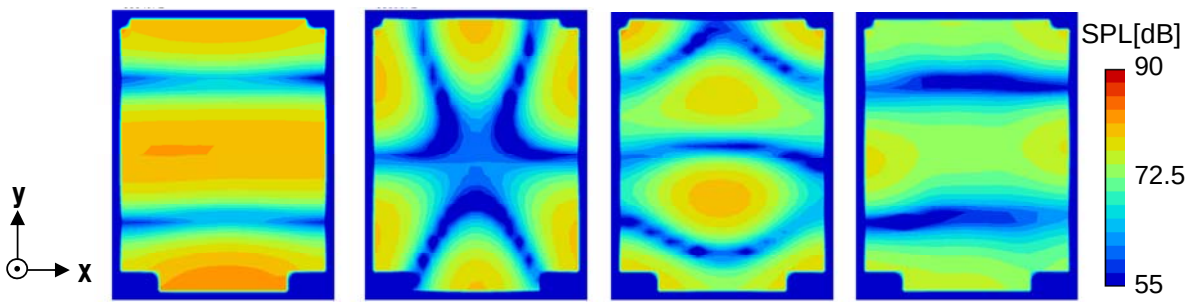

Figure 7 –Distribution of calculated sound pressure level on the floor (50Hz, 69Hz, 74Hz, and 82Hz)

3.2 Optimal Arrangement of ANC System

Numerical simulation utilizing BEM was used for optimal arrangement of ANC system. In this study, the effect of the ANC system was calculated by the following procedures:

1. Calculate sound field by primary sources. In this case, measured vibration acceleration data on the windows was used for calculating the sound field.
2. Calculate sound field by a secondary source which is assumed a point source. In this study, 495 case of sound field were calculated, when a secondary source was installed at 9 points toward x-axis, 11 points toward y-axis, and 5 points toward z-axis, respectively.
3. Modify the absolute value and the phase of the secondary sound to adjust the sound pressure to 0 Pa at the position of the error sensor, and synthesize the primary sound and the secondary sound. In this study, the position of the error sensor was evaluated about 495 cases for each positions of the secondary source. By this process, an optimal position of the error sensor for each positions of the secondary source can be found.

By this simulation, the optimal position of ANC system for decreasing mean-square sound pressure level in the room was found. We focused on the position of secondary source, because the position of the secondary source is the most important for mitigating standing wave. The mean-square sound pressure level in the condition that ANC was operating was calculated, when the secondary source was installed at 495 positions, respectively. And the error sensor was installed at an optimal position according to the position of the secondary source. Figure 8 shows the reduction of mean-square sound pressure levels by operation of the ANC, when the secondary source is installed at the coordinate of this figure. Figure 8 shows the relation between the position of the secondary source and the reduction of mean-square sound pressure levels by operation of ANC. Referring to the Fig.8, the position of the secondary source and the error sensor were determined as shown in Table 3. The secondary source was placed at loop of the standing wave at both frequencies.

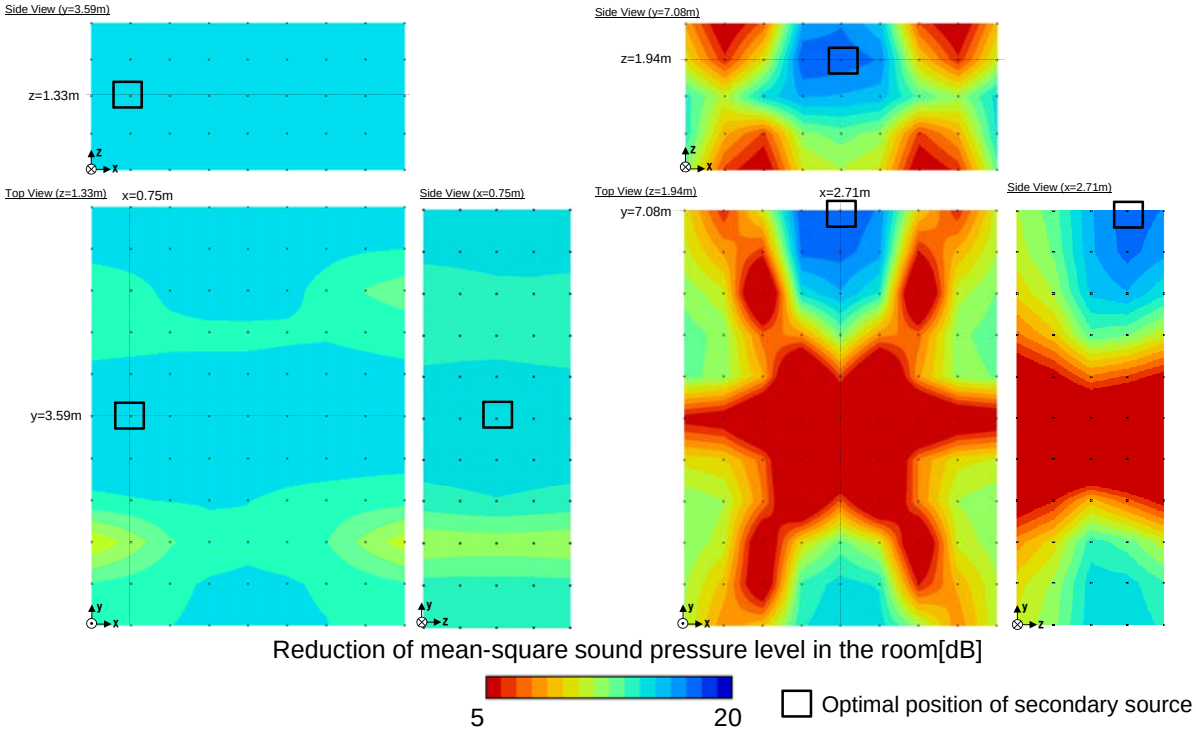

Figure 8 – Reduction of mean-square sound pressure levels by operation of ANC, when the secondary source is installed at the coordinate of this figure.

Table 3 – Position of secondary source and error sensor

	50Hz			69Hz		
	x	y	z	x	y	z
Secondary source	0.75	3.59	1.33	2.71	7.08	1.94
Error sensor	4.01	3.59	1.33	5.32	4.99	1.33

4. EXPERIMENTAL EVALUATION OF ANC

4.1 Experimental Conditions

In this experiment, a feed-forward ANC system was used. The ANC system consists of one speaker, one error sensor, and one reference sensor. The devices used for this experiment are listed in Table 4, and the control conditions of ANC are listed in Table 5. A pure tone is generated from the primary source located outside of the room. An accelerometer, which is acted as a reference sensor, was attached on the window as shown in Fig.2. The sound pressure on the floor was measured at 99 points as shown in Fig.1.

Table 4 – Conditions used for evaluating the mitigating effect of ANC

Application	Device	Manufacturer, model number
Primary source	Loudspeaker	FOSTEX, FW208N
Secondary source	Loudspeaker	FOSTEX, FW208N
Error sensor	Microphone	audio-technica, AT9904
Reference sensor	Accelerometer	Rion, PV-42

Table 5 – Experimental Conditions of ANC system

Algorithm of ANC	Filtered-x LMS
Sampling frequency	4000Hz
Tap length	512

4.2 Results

Figures 9 and 10 show the distribution of sound pressure level at the condition without and with ANC at 50Hz and 69Hz on the floor. Figure 11 shows a histogram of sound pressure levels in the room. Figure 12 shows the maximum, minimum, and mean-square sound pressure level in the room. By comparing Fig.9 and 10, it is confirmed that the loops that existed at the condition without ANC are diminished at the condition with ANC. The disappearance of loops of the eigenmodes can be confirmed in Fig.11 as well. The peak around 90dB existed at the condition without ANC shifted to a lower sound pressure level range by operation of the ANC, indicating that the peak around 90 dB consisted of diminished loops. At a point closest to the error sensor, sound pressure level is decreased 26.4dB at 50Hz, and 19.7dB at 69Hz by operation of the ANC. As shown in Fig.12, ANC decrease all values; maximum, minimum, and mean-square sound pressure. From the above results, it can be confirmed that the single channel ANC system can efficiently reduce noise that is enhanced by a standing wave in the room.

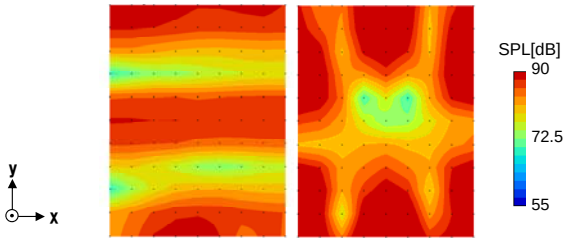

Figure 9 –Distribution of sound pressure level in condition without ANC. (Left:50Hz, Right:69Hz)

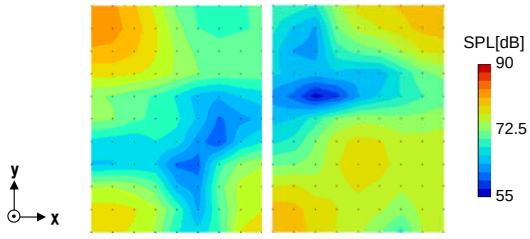

Figure 10 –Distribution of sound pressure level in condition with ANC. (Left:50Hz, Right:69Hz)

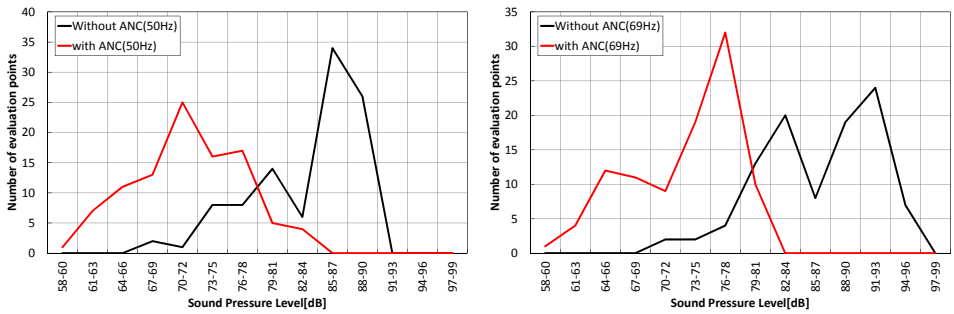

Figure 11 –Histogram of sound pressure level in condition without and with ANC. (Left:50Hz, Right:69Hz)

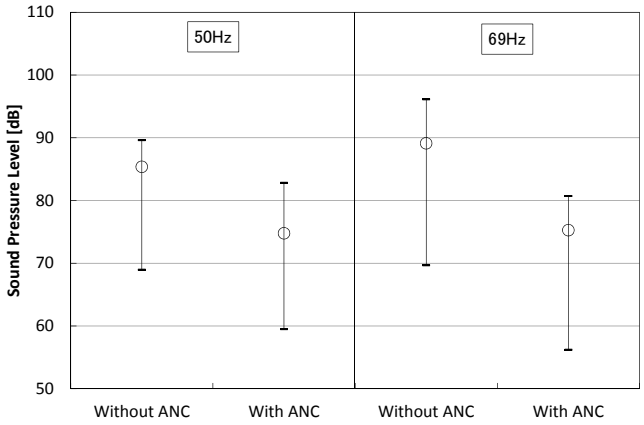

Figure 12 –Maximum, minimum and mean-square sound pressure level in the room.

5. APPLICATION FOR MULTIPLE MODES

5.1 Experimental Conditions

It was confirmed that a single channel ANC system can decrease pure tonal noise that is enhanced by a standing wave. However, there is multiple eigenmodes in enclosed spaces and multiple standing waves may enhance noise simultaneously. Therefore, noise reduction effects of the single channel ANC system against multiple standing waves were evaluated. Arrangement of the ANC system was determined by simulation utilizing BEM as explained in chapter 3. The determined position of the secondary source and the error sensor is shown in Table 6. Synthesized pure tones at 50 Hz, 69Hz, 74 Hz and 82Hz were generated from the primary source. Sound pressure was measured at 9 points toward x-axis, 11 points toward y-axis, and 5 points toward z-axis for a total of 495 points.

Table 6 – Position of secondary source and error sensor

	x	y	z
Secondary source	2.70	0.10	1.95
Error sensor	0.10	6.80	0.70

5.2 Results

Figures 13 and 14 show the distribution of measured sound pressure level without and with ANC on the floor. Figure 15 shows the histogram of sound pressure levels in the room. Figure 16 shows the maximum, minimum, and mean-square sound pressure level in the room. As shown in Fig.13 and 14, the loops that existed at the condition without ANC were diminished at the condition with ANC. As shown in Fig.15, the peak around 80dB existed without ANC shifted to around 70dB by operation of the ANC. As shown in Fig.16, the maximum and mean-square sound pressure was reduced. It was confirmed that the single channel ANC system can reduce noise at resonance frequency in the room efficiently, even in the presence of multiple standing waves.

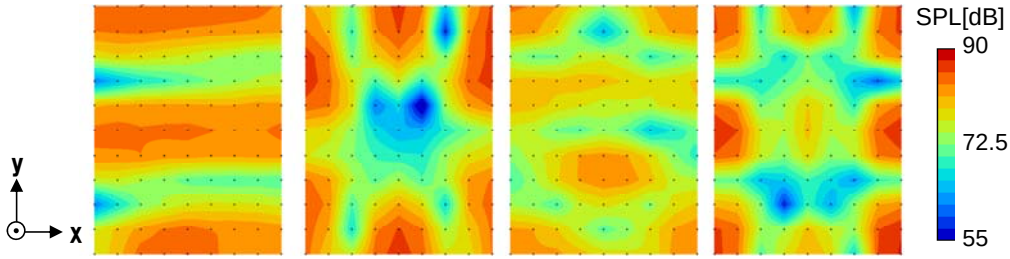

Figure 13 –Distribution of sound pressure level in condition without ANC. (50Hz, 69Hz, 74Hz, and 82Hz)

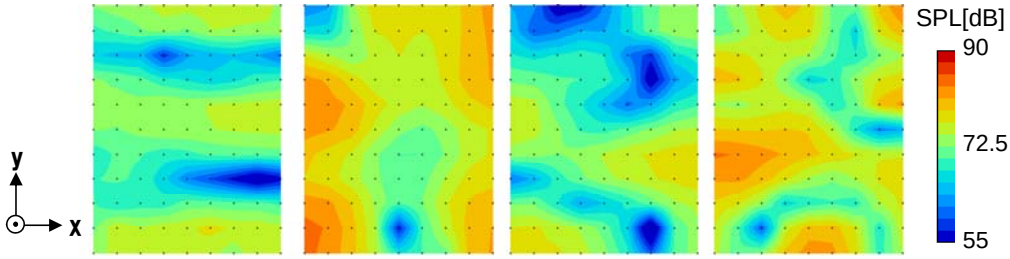

Figure 14 –Distribution of sound pressure level in condition with ANC. (50Hz, 69Hz, 74Hz, and 82Hz)

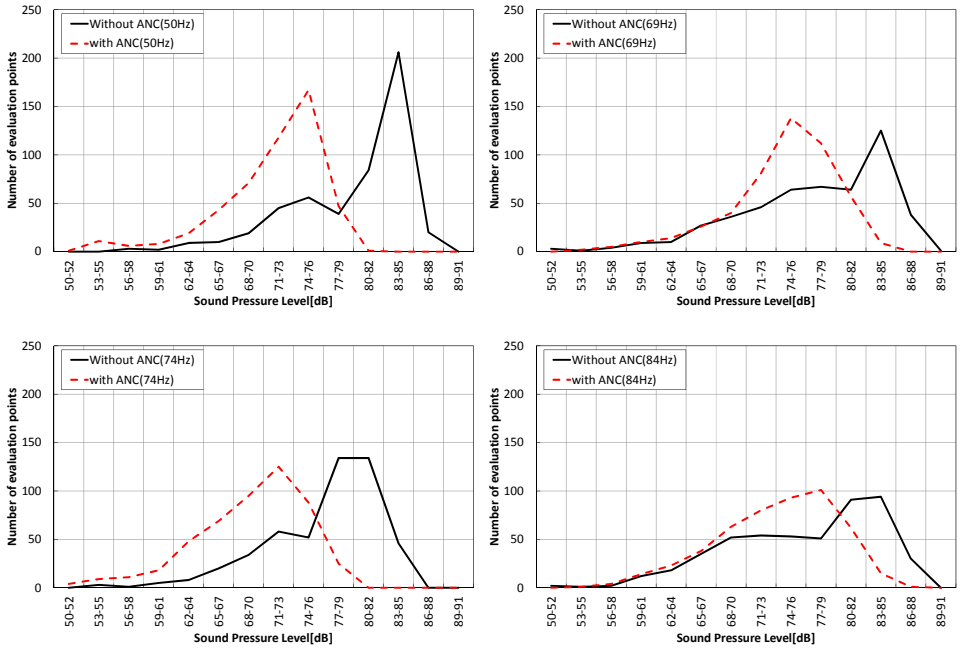

Figure 15 –Histogram of sound pressure level in condition without and with ANC

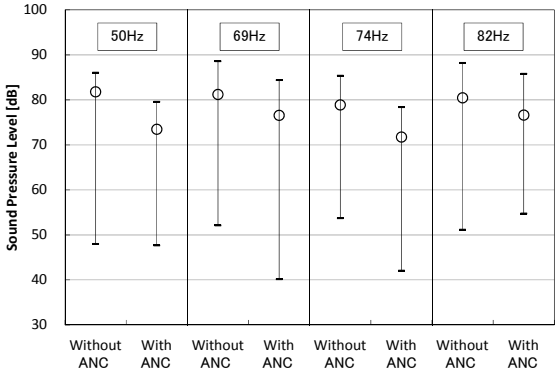

Figure 16 –Maximum, minimum and mean-square sound pressure level in the room.

6. CONCLUSIONS

In this study, the single channel ANC system that has only one secondary source was evaluated. It was confirmed that single channel ANC system can effectively reduce low-frequency noise enhanced by a standing wave, and the effect against the noise on loops of the standing wave were particularly effective. The single channel ANC system can reduce noise at resonance frequency in the room efficiently, even in the presence of multiple standing waves. It was confirmed that numerical simulation utilizing the boundary element method can predict sound fields and can be used for arranging an optimal position of ANC systems.

REFERENCES

1. S.J. Elliott, P.A. Nelson. Active Noise Control, IEEE Signal Process Mag.,10; 1993. p. 12-35.
2. S. Hisashi. Modern advancements in passive and active noise and vibration control technology in automobiles. Proc INTER-NOISE 2011; 4-7 September 2011; Osaka, Japan 2012. 440079.
3. A. Enamito, T. Hayashi, N. Tanaka. A study on Active Noise Control in an Enclosure for Minimizing Total Acoustic Power : Proposal for Acoustic Power Control Using Sound Pressure Attenuation Method. Transactions of the Japan Society of Mechanical Engineers, Series C, Vol.68, No. 672, p 2308-2315.
4. T.Hiruma, A. Enamito, O. Nishimura. A study of sound field control technology to produce both increased area and maintained area in sound pressure. Proc. of 22-th JSME Symposium on Environmental Engineering; Sendai, Japan 2012,pp.14-17.
5. N. Mori, A. Omoto. Study on application of active control in an enclosed sound field - Towards a realization of the ANC system with moving control points-. Proc. ASJ Autumn Meeting; Chiba, Japan 2008, p.687-690.
6. K. Kaneuchi, K. Nishimura, Reduction of low-frequency resonance utilizing active noise control system in enclosed three-dimensional space. Proc. INTER-NOISE 2012; 19-22 August 2012; New york city, USA 2012. 508.